Egyptian Journal of Petroleum (2012) **21**, 101–107

Egyptian Petroleum Research Institute

Egyptian Journal of Petroleum

www.elsevier.com/locate/egyjp
www.sciencedirect.com

FULL LENGTH ARTICLE

Synthesis of carbon nanotubes by CCVD of natural gas using hydrotreating catalysts

Ahmed E. Awadallah *, Sohair M. Abdel-Hamid, Doaa S. El-Desouki, Ateyya A. Aboul-Enein, Ahmed K. Aboul-Gheit

Process Development Division, Egyptian Petroleum Research Institute, Nasr City, Egypt

Received 21 August 2011; accepted 13 December 2011
Available online 3 January 2013

KEYWORDS

Carbon nanotubes;
CCVD;
Hydrotreating;
Ni;
Co;
Mo;
Alumina

Abstract Carbon nanotubes have been successfully synthesized using the catalytic chemical vapor deposition (CCVD) technique over typical refining hydrotreating catalysts (hydrodesulfurization and hydrodenitrogenation) containing Ni–Mo and Co–Mo supported on Al_2O_3 catalysts at 700°C in a fixed bed horizontal reactor using natural gas as a carbon source. The catalysts and the as-grown CNTs were characterized by transmission electron microscopy, HRTEM, X-ray diffraction patterns, EDX and TGA–DTG. The obtained data clarified that the Ni–Mo catalyst gives higher yield, higher purity and selectivity for CNTs compared to Co–Mo catalyst. XRD, TEM and TGA reveal also that the Ni–Mo catalyst produces mostly CNTs with different diameters whereas the Co–Mo catalyst produces largely amorphous carbon.

1. Introduction

Carbon nanotubes (CNTs) are one of the key materials in nanotechnology and are currently among the most intensively investigated materials. However, to supply a variety of commercial applications, the large-scale synthesis of CNTs is still a great challenge. Numerous researchers are devoted to developing various syntheses of CNTs, including laser ablation [1], template synthesis [2], chemical vapor deposition [1,3], and arc discharge [4]. Among the syntheses, catalytic chemical vapor deposition (CCVD) is the most widely employed method because of its direct control on the reaction parameters such as catalyst system, temperature, composition, and flow rate of carbon precursor–carrier and hydrocarbon [5]. Accordingly, CCVD is expected to be the most popular method for large-scale production of carbon nanostructures.

As for CNT formation, transition metal (e.g., Ni-, and Co-supported catalysts) and hydrocarbons (e.g., methane, ethane, acetylene, ethylene, carbon monoxide, and other synthesis gas) have been used in CCVD synthesis of CNT products [6–12]. Another operating parameter, the selection of supporting materials, also plays a crucial role in determining the growth of CNTs in a fluidized bed reactor because it would affect productivity, structural characteristics and purity of CNT products [13]. The type of supports including Al_2O_3,

* Corresponding author. Tel.: +20 2 24103421; fax: +20 2 2747433.
E-mail address: ahmedelsayed_epri@yahoo.com (A.E. Awadallah).

Peer review under responsibility of Egyptian Petroleum Research Institute.

ELSEVIER Production and hosting by Elsevier

1110-0621 © 2012 Egyptian Petroleum Research Institute. Production and hosting by Elsevier B.V. Open access under CC BY-NC-ND license.
http://dx.doi.org/10.1016/j.ejpe.2012.11.005

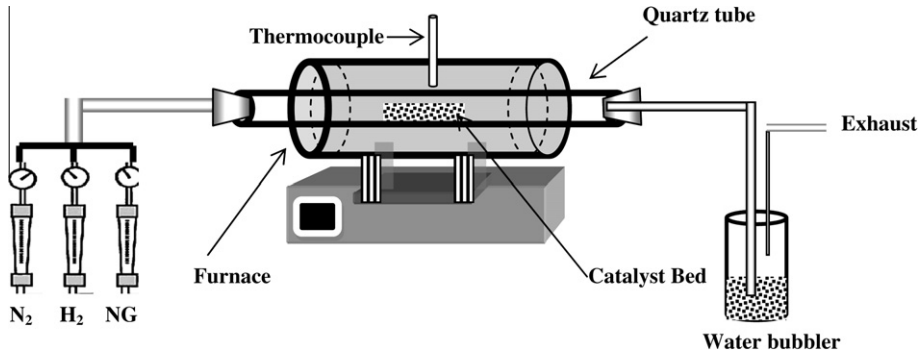

Figure 1 A typical schematic diagram of a natural gas decomposition reactor system.

SiO_2, MgO, and zeolite are the most investigated in the past literature.

Successful examples have confirmed the effectiveness of bimetallic catalysts in the synthesis of thin-walled CNTs, such as Fe/Mo [14], Ni/Mo [15–17], Co/Mo [18], and Fe/Co [19] catalysts. For the potential catalytic action of Ni/Mo/MgO for thin-walled CNT synthesis [15], Li et al. [16] prepared Ni/Mo/MgO catalyst with the combustion method, which has a 8000% yield per gram of catalyst for multi-walled CNTs. Shimizu et al. [17] obtained cone-shaped CNT assemblies with Ni/Mo catalyst sputtered on a silicon wafer. However, the loading of metals on supports is still high (i.e. 5% mole fraction of Ni/Mo loading in previous study) [14–22].

The present work aims to evaluate the catalytic growth activity of CNTs using traditionally hydrotreating nickel or cobalt molybdate supported on alumina catalysts that are already used for the hydrodesulfurization (HDS) and hydrodenitrogenation (HDN) processes of petroleum fractions. Also the use of natural gas as a feed stock, which is an extremely cheap source of carbon and great availability that leads to the low-cost production of carbon nanotubes.

2. Experimental

2.1. Activation of the catalysts

A commercial un-sulfided hydrotreating Ni–Mo and Co–Mo/Al_2O_3 catalysts were kindly provided by Suez Petroleum Co., Suez City, Egypt. Before carrying out the catalytic runs; the catalysts were activated via drying at 120°C overnight then calcined in air at 550°C for 3 h. The typical compositions of the composite catalysts are 5.2 wt% NiO–10.96 wt% MoO and 3.1 wt% CoO–10.5 wt% MoO/Al_2O_3.

Table 1 Typical composition of natural gas feed stock.

Component	Percent, wt%
Methane	89.48
Ethane	7.46
Propane	1.86
iso-Butane	0.46
n-Butane	0.36
iso-Pentane	0.18
n-Pentane	0.071
iso-Hexane	0.076
n-Hexane	0.049

2.2. Synthesis of CNTs

In a typical synthesis, the catalyst powder of 0.5 g was dispersed on a porcelain boat of 10 cm length and placed in the center of a quartz tube with a diameter of 35 mm and 100 cm length fitted within a horizontal furnace (Fig. 1). The temperature was increased to 500°C under hydrogen gas flow of 20 ml/min and kept at this temperature for 2 h to deoxidize the catalyst, beyond which the temperature was increased again to 700°C under N_2 flow of 50 ml/min. After temperature equilibration was reached, natural gas (25 ml/g/min) was introduced into the quartz tube for a certain reaction time of 60 min. A typical composition of natural gas feed stock is depicted in Table 1.

2.3. Materials characterization

2.3.1. Transmission electron microscope (TEM)

Carbon nanotube diameters and morphology have been determined by transmission electron microscopy (TEM, Model JEM-200CX, JEOL, Japan). A small quantity of used catalysts were dispersed in 10 ml ethylene glycol and sonicated for 10 min. A few drops of the resulting suspension were placed on a covered copper grid.

2.3.2. X-ray diffraction patterns (XRD)

Powder X-ray diffraction experiments were performed for the current catalysts before and after the catalytic runs using X'Pert PRO MPD PANalytical. The patterns were recorded using CuKα radiation (λ = 0.1541 nm) and 2θ ranging from 10° to 85°.

2.3.3. Thermo-gravimetric analysis (TGA) and differential thermal analysis (DTA)

TGA and DTA were performed using SDT; Q600 apparatus using 20 mg catalyst samples at a heating rate of 10°C min^{-1} in an air flow of 50 cm^3/min. Carbon yield for each catalyst was calculated using the following equation:

$$\text{Carbon yield} = (\%\ \text{weight loss by carbon oxidation}/\%\ \text{of residue after oxidation}) \times 100\%.$$

3. Results and discussion

Fig. 2 shows TEM pictures of CNTs grown at 700°C in a fixed bed horizontal quartz tube reactor for 1 h over Ni–Mo/Al_2O_3

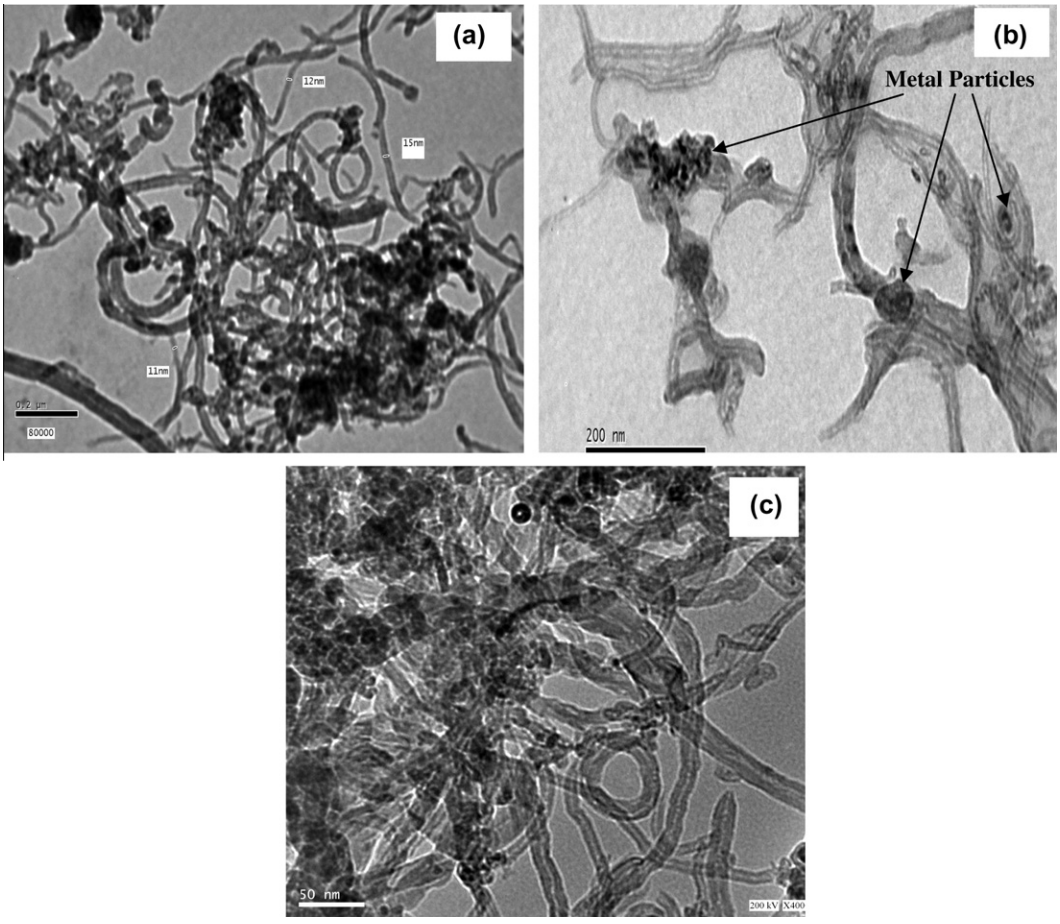

Figure 2 TEM images of CNTs growth over Ni–Mo/Al_2O_3 catalyst at different positions (a and b) scale bar 200 nm and (c) scale bar 50 nm.

catalyst. The morphology of the CNTs illustrates that the CNTs formed under these conditions are entangled with each other and possess curved, hollow, and tubular shapes, with diameters in the range of ~8–15 nm. Beside CNTs production on the Ni–Mo catalyst, some amorphous carbon and metal particles were also detected as shown in Fig. 2a. The diameters of the produced CNTs are somewhat smaller than the sizes of the catalyst particles (Fig. 2b). Also, some catalyst particles appear to be encapsulated within the nanotubes hollow core.

Fig. 3 shows the as-synthesized CNTs in presence of the Co–Mo/Al_2O_3 catalyst at the same reaction conditions. It is evident that a lower yield and selectivity of CNTs occurs; where a wide distribution of CNT diameters appears (from ~5 to 35 nm) on the surface of the metal particles of this cat-

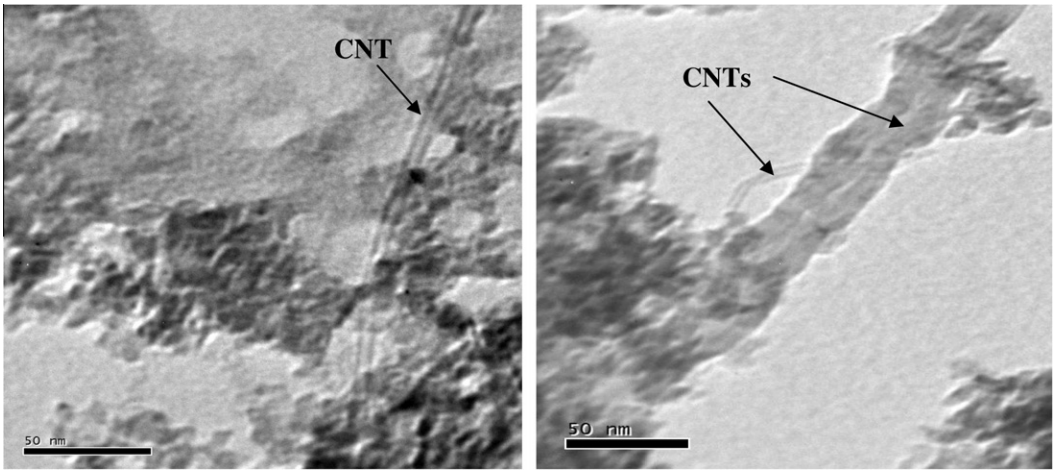

Figure 3 TEM images of CNTs growth over Co–Mo/Al_2O_3 catalyst at different positions (scale bar 50 nm).

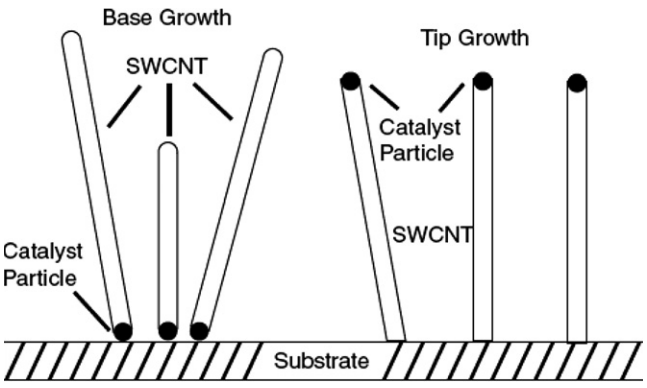

Figure 4 Base growth (left) and tip growth (right) mechanisms.

alyst besides, a considerable amount of amorphous carbon adhering to the outside layer of CNTs.

Usually, Mo has been reported to present synergism when combined with other transition metals in bimetallic catalysts, leading to a drastic effect on both yield and morphology of the as-produced CNT bundles. This confirms that Mo is absolutely necessarily for the preparation of CNT bundles. Tang et al. [23] had systematically investigated the influence of the different ratios of Mo and Co on the synthesis of CNTs. They observed that the addition of Mo to Co/MgO obviously increased the yield of CNTs.

Metal catalysts with Mo, such as Ni/Mo/MgO, Ni–Y/Mo, $Mg_{1-x}Fe_xMoO_4$ and $MgMoO_4$ [16,24–27], were used to prepare the CNT bundles by catalytic chemical vapor deposition method with methane as the carbon source. Mo has been reported to have a drastic effect on both the yield and the morphology of the CNT bundles and to be necessary for their preparation. Jia et al. [28] have successfully fabricated MWCNT using Mo/MgO catalyst without any addition of an active component i.e., Fe, Co or Ni. Furthermore, several authors accepted that the addition of Mo in the catalyst system can increase CNT yield in a large scale [29,30].

Another aspect about the role of Mo metal as an ideal promoter for catalyzing the decomposition of hydrocarbons into carbon nanostructured materials is the great ability of this metal oxide to be reduced into Mo carbides at the initial stage of the reaction. It is well established and documented that molybdenum is known to be the most promising catalytic center for enhancing the aromatization of methane under non-oxidative conditions [31]. Aboul-Gheit and Awadallah observed that natural gas was completely decomposed to C especially Mo_2C and H_2 over 6 wt%Mo/H-ZSM5 promoted with Pd, Ir, Cr or W catalysts at 5 min time-on-stream [32,33]. These carbides could continually provide the active centers i.e., Ni or Co by carbon before the nucleation step. This suggests that the presence of Mo may facilitate the solubilization of carbon on the surface of Ni or Co particles on the catalyst. Nakamura et al. [15] stated that the Mo carbide and Ni play different roles in the synthesis of the thin CNTs, in which Ni is responsible for the dissociation of CH_4 into carbon and Mo_2C that works as a carbon reservoir.

According to the two widely accepted 'tip-growth' and 'base-growth' mechanisms [34], the hydrocarbon gas decomposes on the surfaces of the metal particle to release carbon (Fig. 4). The carbon atoms will dissolve in these metal particles and diffuse through the particle, resulting in the precipitation of the filament. Moreover, the metal–support interactions are found to play a determinant role for the growth mechanism [31,35]. Weak interactions yield tip-growth mode whereas strong interactions lead to base-growth. Both growth modes are schematically shown in Fig. 4. Based on these findings, the growth of CNTs over Ni–Mo/Al_2O_3 catalyst proceeds via the base mechanism; indicating that there is a strong interaction between metal particles and support in this catalyst (Fig. 5).

HRTEM analysis shows that the produced carbon nanotubes are multi-walled as can be seen in Fig. 5b. Moreover, the hollow tip without catalytic particle is very regular. The sharp fringe of the walls indicates the good crystallinity of graphite sheets. It is also evident from Fig. 5b that the end of CNT is free from the metal particles, which emphasizes the base growth mechanism over the Ni–Mo catalyst.

The EDX spectrum of the current Ni–Mo catalyst after the growth of CNTs shows a distinct C peak; indicating the higher content of deposited carbon on this catalyst (Fig. 6a). However, using the Co–Mo catalyst for production of CNTs; a considerable drop in carbon content is observed (Fig. 6b). These variations reveal that the Ni–Mo catalyst possesses faster as well as higher ability to dissociate natural gas hydrocarbon components compared to the corresponding Co–Mo catalyst. Tian et al. [35] also observed that the Ni-containing catalyst has a faster deposition rate of carbon atoms and leads to a much higher carbon yield than other active components such as Fe and Co.

XRD analysis is an important tool used for clarifying the as-synthesized CNTs in the catalysts. XRD patterns of Ni–Mo catalysts before and after CNT growth are depicted in Fig. 7a and b, respectively. It is clearly shown that the peaks at *ca.* $2\theta = 26$ and 44° correspond to graphite, which is attributed to the graphitic structure of CNTs (Fig. 7b). The intensities of these peaks are somewhat higher than the remaining peaks attributed to metal oxides in the catalyst. It is logically expected that the CNT growth at high temperature would favor the graphitization degree. This evidently indicates that the Ni–Mo catalyst exhibits higher activity for production of CNTs in spite of the higher Mo content against the most active Ni particles (10.96 vs. 5.20 wt%, respectively). This also indicates that CNTs are well graphitized using Ni–Mo catalyst.

In contrast, the Co–Mo catalyst shows insignificant activity toward the CNTs growth. The physical appearance of this catalyst after the catalytic run was completely dark black and mainly a fine rough powder, whereas the carbon deposit on Ni–Mo was soft and spongy. The XRD patterns show the disappearance of graphite peaks at principally $2\theta = 26$ (Fig. 8b) using Co–Mo/Al_2O_3 catalyst. This behavior indicates that the Co–Mo catalyst produces mainly amorphous carbon.

Furthermore, by comparing the XRD patterns of the current catalysts before carrying out the catalytic growth of CNT (Figs. 7a and 8a); one can see that the peaks of Mo–Co/Al_2O_3 catalyst are somewhat wider than those of Mo–Ni/Al_2O_3, reflecting a lower crystallite size of the Ni containing catalyst. The lower crystallite size could enhance the catalytic activity via increasing both surface area as well as metal dispersion.

TGA analysis is employed to examine the thermal stability and purity of as-grown CNTs using the current catalysts. A general way to estimate the quantity of the deposited carbon

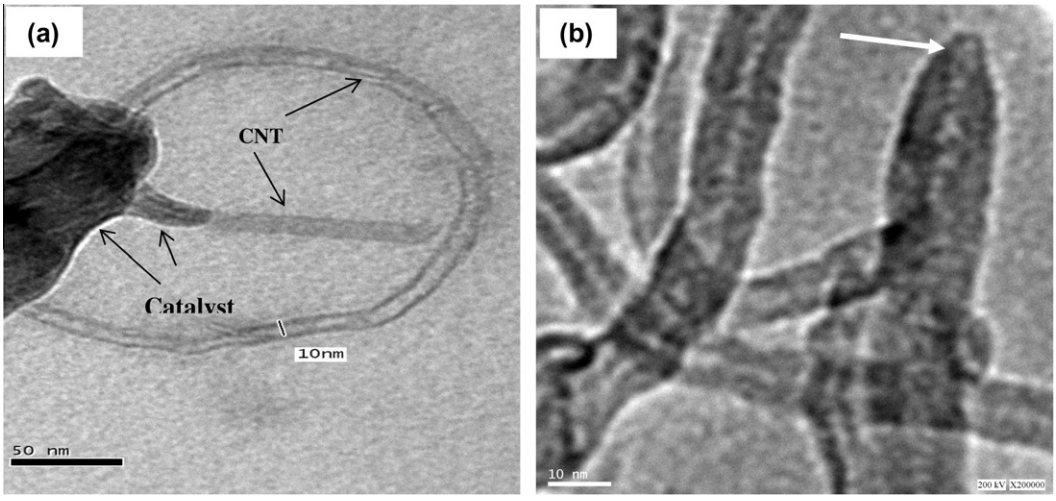

Figure 5 (a) TEM image showing base-growth of CNTs using Ni–Mo/Al_2O_3 catalyst and (b) HRTEM of CNTs over Ni–Mo/Al_2O_3 catalyst.

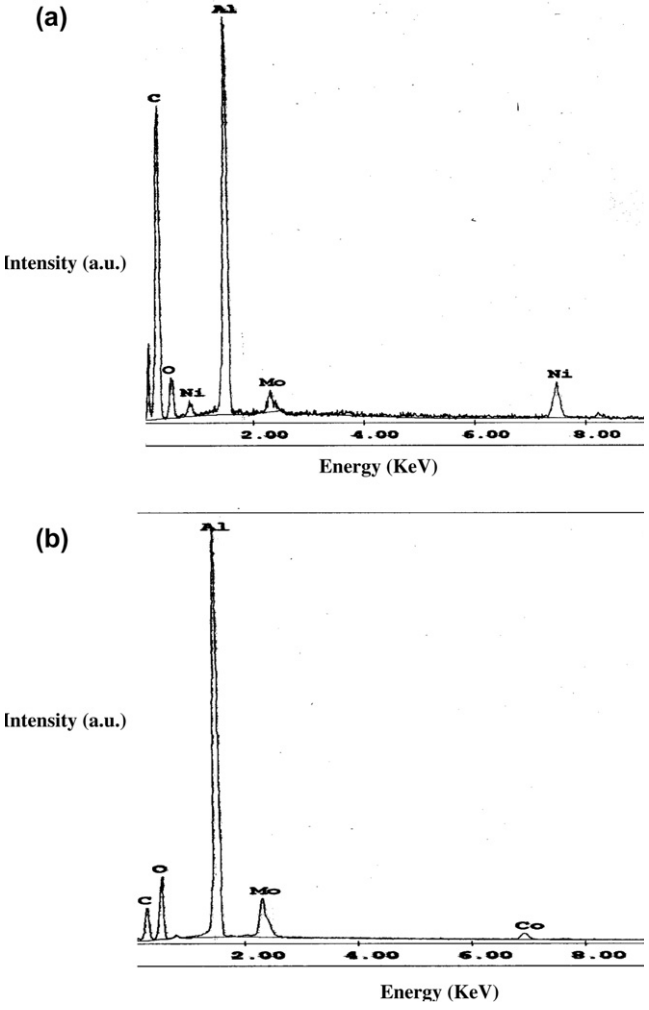

Figure 6 EDX spectrum of Ni–Mo catalyst (a) and Co–Mo catalyst (b) after CNT growth.

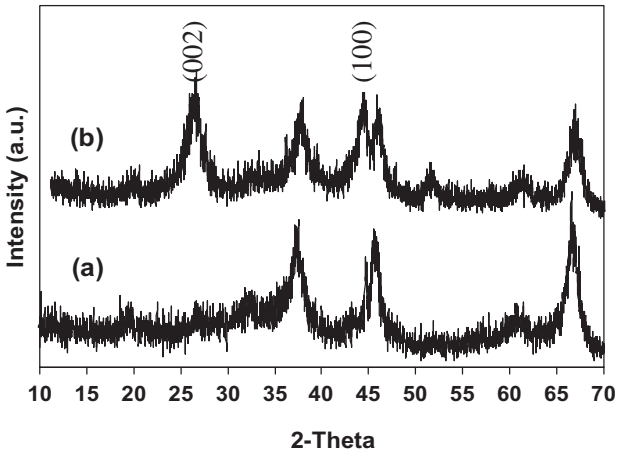

Figure 7 XRD patterns of Ni–Mo/Al_2O_3 before (a) and after (b) growth of CNTs.

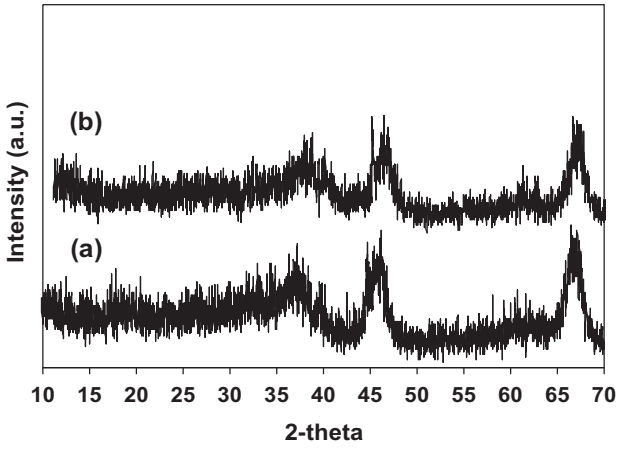

Figure 8 XRD patterns of Co–Mo/Al_2O_3 before (a) and after (b) the growth of CNTs.

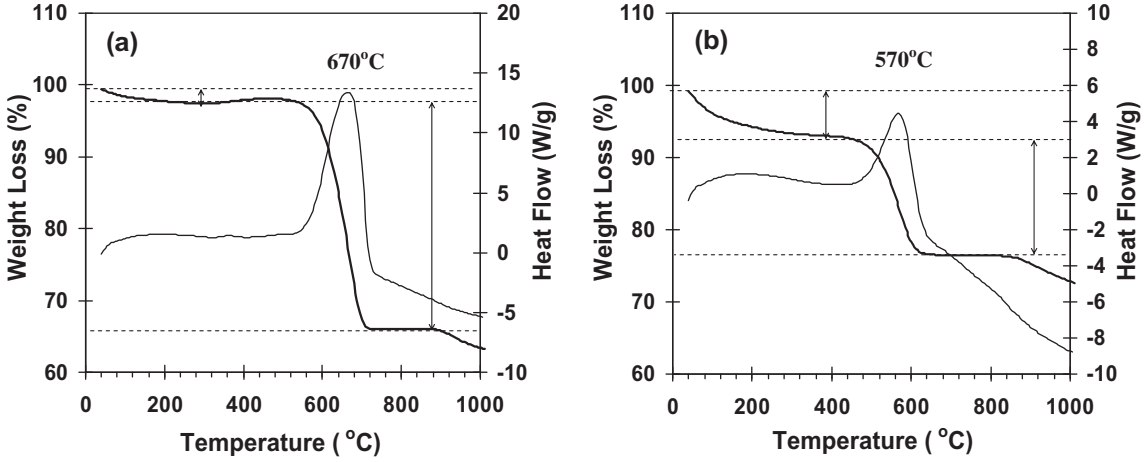

Figure 9 TGA and DTG of (a) Ni–Mo/Al_2O_3 and (b) Co–Mo/Al_2O_3 catalysts after the growth of CNTs.

during the decomposition of hydrocarbon molecules on the catalysts by CCVD is the direct weight of the catalyst before and after the reaction; but, this method is subject to high experimental errors since both the initial catalyst powder as well as the carbon–catalyst composite can be lost during the experimental process. The use of thermogravimetric analysis (TGA) permits for a more accurate determination of the deposited carbon [16]. The weight loss due to the combustion of carbon begins at temperatures of $\geqslant$300°C depending on the nature of the carbon species [16,36].

Fig. 9a and b shows the weight loss and derivative weight curves for as-grown CNTs over Ni- and Co-catalysts, respectively. It is evident that the two catalysts presented a similar oxidation behavior, with a single step degradation, however, the Co–Mo catalyst showed a considerable mass loss from the initial heat treatment stage up to ~450°C compared to the Ni–Mo catalyst, and this occurred mainly due to the presence of both physisorbed moisture and amorphous carbon in the CNT walls [36]. Moreover, in the DTG curves, the combustion temperature of CNTs over the Ni containing catalyst (~670 °C) is higher than that over the Co containing catalyst (~570 °C) (Fig. 9). We observed also that the inflection temperature and end temperature of Ni- and Co- containing catalysts are 550–700 and 450–610 °C; respectively, which illustrate that the CNTs produced by Ni–Mo catalyst possess a higher quality and degree of graphitization. Chen et al. stated that the higher the inflection temperature and the smaller difference between the on-set and end temperature indicate the presence of highly graphitized MWCNTs [37]. These data indicate that the Ni–Mo catalyst produces CNTs with higher graphitization degree, higher thermal stability, higher purity as well as lower defects around the sides of tubes.

Furthermore, the efficiency of catalysts to grow CNTs can be reflected by the weight loss of the carbon deposits, hence, according to calculations, the yield of the CNT amount to 55.01 and 33.38 wt% for the samples obtained by the Ni–Mo and Co–Mo catalysts, respectively (Fig. 9a and b).

4. Conclusion

High quality carbon nanotubes were successfully prepared by using the catalytic decomposition of natural gas over Ni–Mo and Co–Mo supported on Al_2O_3 catalysts in a fixed bed horizontal reactor. TEM, XRD and TGA–DTG analysis indicated that the Ni-containing catalyst exhibited higher activity and faster decomposition of natural gas compared to the Co-containing catalyst. The Ni–Mo catalyst produced CNTs with higher thermal stability and purity whereas the Co–Mo catalyst produced largely amorphous carbon.

Acknowledgment

The authors would like to thank Prof. Dr. Ahmed M. El-Sabbagh, Director of the Egyptian Petroleum Research Institute (EPRI) for his interest and sincere assistance besides the provision of the instruments and chemicals necessary for carrying out this work.

References

[1] T. Guo, P. Nikolaev, A. Then, D.T. Colbert, R.E. Smalley, Chem. Phys. Lett. 243 (1995) 49–54.
[2] C.-T. Hsieh, J.-M. Chen, R.-R. Kuo, Y.-H. Huang, Appl. Phys. Lett. 84 (2004) 1186–1188.
[3] J.M. Ting, N.Z. Huang, Carbon 39 (2001) 835–839.
[4] T.W. Ebbesen, P.M. Ajayan, Nature 358 (1992) 220–222.
[5] A.R. Biris, A.S. Biris, D. Lupu, S. Trigwell, E. Dervishi, Z. Rahman, P. Marginean, Chem. Phys. Lett. 429 (2006) 204–208.
[6] M. Corrias, B. Caussat, A. Ayral, J. Durand, Y. Kihn, P. Kalck, P. Serp, Chem. Eng. Sci. 58 (2003) 4475–4482.
[7] W. Qian, T. Liu, Z. Wang, F. Wei, Z. Li, G. Luo, Y. Li, Appl. Catal. A 260 (2004) 223–228.
[8] Y. Wang, F. Wei, G. Luo, H. Yu, G. Gu, Chem. Phys. Lett. 364 (2002) 568–572.
[9] D. Venegoni, P. Serp, R. Feurerb, Y. Kihnc, C. Vahlas, P. Kalck, Carbon 40 (2002) 1799–1807.
[10] G. Luo, Z. Li, F. Wei, L. Xiang, X. Deng, Y. Jin, Physica B 323 (2002) 314–317.
[11] H. Yu, Q. Zhang, F. Wei, W. Qian, G. Luo, Carbon 41 (2003) 2855–2863.
[12] W. Qian, T. Liu, F. Wei, Z. Wang, Y. Li, Appl. Catal. A 258 (2004) 121–124.
[13] J.P. Cheng, X.B. Zhang, Z.Q. Luo, F. Liu, Y. Ye, W.Z. Yin, W. Liu, Y.X. Han, Mater. Chem. Phys. 95 (2006) 5–11.
[14] W.Z. Qian, T. Liu, F. Wei, Carbon 41 (2003) 846–848.

[15] L.-P. Zhou, K. Ohta, K. Kuroda, N. Lei, K. Matsuishi, L. Gao, T. Matsumoto, J. Nakamura, J. Phys. Chem. B 109 (2005) 4439–4447.
[16] Y. Li, X.B. Zhang, X.Y. Tao, J.M. Xu, W.Z. Huang, J.H. Luo, Z.Q. Luo, T. Li, F. Liu, Y. Bao, H.J. Geise, Carbon 43 (2005) 295–301.
[17] Y. Shimizu, T. Sasaki, T. Kodaira, Chem. Phys. Lett. 370 (2003) 774–780.
[18] J.E. Herrera, B. Leandro, B. Armando, J. Catal. 204 (2001) 129–145.
[19] P. Coquay, E. Flahaut, E. DeGrave, J. Phys. Chem. B 109 (2005) 17825–17830.
[20] B. Lukic, J.W. Seo, R.R. Bacsa, Nano Lett. 5 (2005) 2074–2077.
[21] N. deJonge, M. Allioux, M. Doytcheva, Appl. Phys. Lett. 85 (2004) 1607–1609.
[22] I. Willems, Z. Konya, J.F. Colomer, Chem. Phys. Lett. 317 (2000) 71–76.
[23] S. Tang, Z. Zhong, Z. Xiong, L. Sun, L. Liu, J. Lin, Z.X. Shen, K.L. Tan, Chem. Phys. Lett. 350 (2001) 19–26.
[24] M. Kadlečíková, A. Vojaćková, J. Breza, V. Luptáková, M. Michalka, K. Jesenák, Mater. Lett. 61 (2007) 4549–4552.
[25] J.M. Xu, X.B. Zhang, Y. Li, X.Y. Tao, F. Chen, T. Li, Y. Bao, H.J. Geise, Diamond Relat. Mater. 13 (2004) 1807–1811.
[26] Y. Li, X.B. Zhang, X.Y. Tao, J.M. Xu, F. Chen, L.H. Shen, X.F. Yang, F. Liu, G. Van Tendeloo, H.J. Geise, Carbon 43 (2005) 1325–1328.
[27] M.G. Donato, S. Galvagno, G. Messina, C. Milone, A. Pistone, S. Santangelo, Diamond Relat. Mater. 16 (2007) 1095–1100.
[28] Y. Jia, L. He, L. Kong, J. Liu, Z. Guo, F. Meng, T. Luo, M. Li, J. Liu, Carbon 47 (2009) 1652–1658.
[29] H.J. Dai, A.G. Rinzler, P. Nikolaev, A. Thess, D.T. Colbert, R.E. Smalley, Chem. Phys. Lett. 260 (1996) 471–475.
[30] M. Motiei, J. Calderon-Moreno, A. Gedanken, Chem. Phys. Lett. 357 (2002) 267–271.
[31] A.M. Cassell, J.A. Raymakers, J. Kong, H. Dai, J. Phys. Chem. B 103 (1999) 6484–6492.
[32] A.K. Aboul-Gheit, A.E. Awadallah, S.M. El-Kossy, A.H. Mahmoud, J. Nat. Gas Chem. 17 (2008) 337–343.
[33] A.K. Aboul-Gheit, A.E. Awadallah, J. Nat. Gas Chem. 18 (2009) 71–77.
[34] R.T.K. Baker, Carbon 27 (1989) 315–323.
[35] F. Tian, H.P. Li, N.Q. Zhao, C.N. He, Mater. Chem. Phys. 115 (2009) 493–495.
[36] C.-M. Chen, M. Chen, F.-C. Leu, S.-Y. Hsu, S.-C. Wang, S.-C. Shi, C.-F. Chen, Diamond Relat. Mater. 13 (2004) 1182–1186.
[37] C. Chen, Y. Dai, J. Huang, J. Jehng, Carbon 44 (2006) 1808–1820.